Small-Angle X-ray Scattering Study of Gelation and Aging of Eu^{3+}-Doped Sol−Gel-Derived Siloxane−Poly(oxyethylene) Nanocomposites

Karim Dahmouche,*,† Luis D. Carlos,‡ Celso V. Santilli,† Verônica de Zea Bermudez,§ and Aldo F. Craievich||

Instituto de Química, Universidade Estadual Paulista, C. P. 355 CEP 14800−900 Araraquara-SP, Brazil, Departamento de Física, Universidade de Aveiro, Aveiro, Portugal, Departamento de Química, Universidade de Trás-os Montes e Alto Douro, Vila Real, Portugal, and Instituto de Física, Universidade de São Paulo, São Paulo-SP, Brazil

Received: October 18, 2001

The aggregation, gelation, and aging of urea-cross-linked siloxane−poly(oxyethylene) nanohybrids [(U600)-*n*] containing two different amounts of europium triflate initially dissolved in an ethanol−water mixture were investigated by in situ small-angle X-ray scattering (SAXS). For both low (n = [O]/[Eu] = 80) and high (n = 25) europium contents, the SAXS intensity was attributed to the formation of siloxane clusters of about 8−11 Å in size. Siloxane cluster formation and growth is a rapid process in hybrids with low Eu contents and slow in Eu-rich hybrids. An additional contribution to the scattering intensity at very low angles was attributed to the formation of a coarse structure level. At this secondary level, the structure can be described as a set of dense domains containing siloxane clusters embedded in a depleted matrix composed of unfolded polymer chains and solvent. By fitting a theoretical function for this model to the experimental SAXS curves, relevant structural parameters were determined as functions of time during the sol−gel transition and gel aging. For hybrids with low europium contents (n = 80), the size of the siloxane clusters remains essentially invariant, whereas the dense segregation domains progressively grow. In hybrids with high doping contents (n = 25), the preponderant structure variation during the first stages of the sol−gel transformation is the slow growth of siloxane clusters. For these hybrids, the segregation of siloxane clusters forming dense domains occurs only during advanced stages of the process.

1. Introduction

The sol−gel process has been successfully used in the past few years for the production of advanced multifunctional materials such as monoliths, thin films, fibers, and powders.[1] This method is particularly adapted to the preparation of organic/inorganic hybrid composites because of the possibility of tailoring compounds by mixing, at around room temperature and at the nanometer scale, organic and inorganic components into a single material.[1−5] The synergy of that combination and the role of the organic/inorganic interface are important obtaining composites exhibiting unusual electrochemical, biological, mechanical, electrical, and optical properties.[2−5] In particular, hybrid photonic materials for optical data storage, optical waveguides, sensors, electrochromic smart windows, solid-state lasers, and screen displays have recently been obtained.[5−8]

A new particularly interesting family of photonic nanocomposites (termed di-ureasils) consists of poly(oxyethylene) (POE) chains of variable length grafted, on both ends, to a siliceous backbone through urea functionalities. The incorporation of lanthanide ions onto the di-ureasil framework leads to the synthesis of multiwavelength nanohybrid emitters, whose emission spectra display a large host band superposed on a series of sharp cation lines.[9−16] The large band results from an uncommon convolution of a contribution arising from the NH groups of the urea bridges with electron−hole recombinations that occur in the nanometer-sized siloxane domains.[17] The excitation wavelength, the amount of Eu^{3+} ions incorporated, and the siloxane domain sizes determine the broad band energy range.[13,15,17] Therefore, a good knowledge of the structural mechanisms involved in the formation of the siloxane nanodomains is essential to the control and optimization of the photoluminescence properties.

Small-angle X-ray scattering (SAXS) is a particularly appropriate technique for studying the structure of nanohybrids because of the disordered nature of these materials and the high contrast of electron densities between the inorganic (siloxane-rich) clusters and the organic (polymer-rich) matrix.[18−24] SAXS studies of the sol−gel transition (gelation) of undoped siloxane−PPO hybrids[18] revealed that these systems exhibit a fractal structure when they are in the sol and wet gel states. After being dried by evaporation of solvent at constant temperature, the material is formed by polymer chains linked by spatially correlated siloxane nanoparticles located at their ends.[18−21]

On the other hand, it was shown that europium doping modifies the structure of the dried siloxane−poly(oxyethylene) hybrids gels by promoting a two-level hierarchical structure.[22] The primary structural level is constituted by siloxane nanoclusters formed by polycondensation reactions between silicon-based species located at the polymer chains ends. The secondary coarse level consists of domains of high average electron density in which siloxane clusters are segregated embedded in a cluster-depleted low-density matrix. Siloxane nanoclusters inside the

* To whom correspondence should be addressed. Fax: (55) (16) 222 79 32. E-mail: karidahm@iq.unesp.br.
† Universidade Estadual Paulista.
‡ Universidade de Aveiro.
§ Universidade de Trás-os Montes e Alto Douro.
|| Universidade de São Paulo.

10.1021/jp013826b CCC: $22.00
Published on Web 04/10/2002

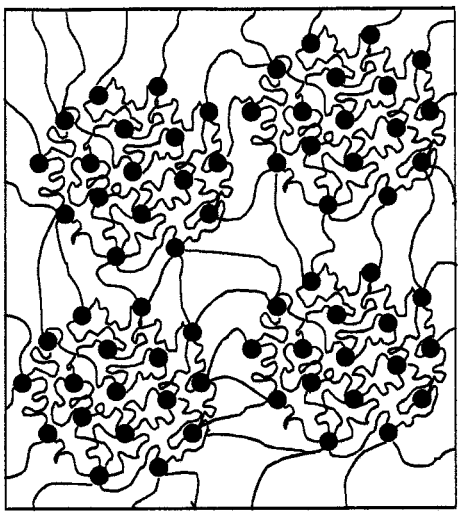

Figure 1. Model of the two-level structure of the Eu^{3+}-doped siloxane−POE hybrid material. Siloxane clusters (black spheres) aggregate in domains that are embedded in a siloxane-depleted matrix.

segregation domains are rather close, so that polymer chains linking clusters belonging to the same domain are expected to be in folded conformations. On the other hand, clusters belonging to different domains are rather far from one another, so the polymer chain linking them are expected to be in nearly unfolded conformations. A schematic picture of this model is shown in Figure 1.

Furthermore, the doping level determines the nature of the Eu^{3+} coordination shell in such materials.[22] As both the Eu^{3+} local structure and the spatial arrangement of the siloxane domains determine the luminescence features of europium-doped dried di-ureasils gels,[22] it appears particularly interesting to establish how the incorporation of Eu^{3+} affects the siloxane clustering processes during and after gelation and to characterize the mechanisms leading to the formation of the two-level hierarchical structure observed in the dried materials.

This work reports a SAXS study of the sol−gel transition and aging of urea-cross-linked siloxane−poly(oxyethylene) hybrids in which two different amounts of europium triflate, $Eu(CF_3SO_3)_3$, were dissolved. Our purpose is to understand how the Eu^{3+} doping level modifies the gelation and aging processes and affects the structure and luminescence emission of the final material.

2. Experimental Procedures

2.1. Sample Preparation. The preparation of the sols used to obtain Eu^{3+}-doped siloxane−POE hybrids has already been described.[9,10,13,15] The covalent bond between the alkoxysilane precursor (3-isocyanatopropyltriethoxysilane, ICPTES) and the oligopolyoxyethylene segment are formed by reacting the isocyanate group of the former compound with the terminal amine groups of doubly functional amines (chemically α,*β*,*γ* *ω*-diaminepoly(oxyethylene-*co*-oxypropylene) and commercially Jeffamine-ED-600) in tetrahydrofuran. A urea-cross-linked organic−inorganic precursor (b = 8.5 and a+c = 2.5 units, respectively) is thus obtained.

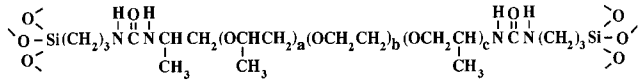

The europium salt, $Eu(CF_3SO_3)_3$, is incorporated during the sol−gel process by dissolving it in ethanol and water (molar proportion 1 ICPES:4 CH_3CH_2OH:1.5 H_2O). The two solvents are used to start the hydrolysis and condensation reactions. The doped siloxane−POE hybrids are designated $U(600)_nEu(CF_3SO_3)_3$, where the number 600 indicates the molecular weight of the polymer and n = [O]/[Eu] represents the ratio of Eu^{3+} ions per ether-type oxygen of the poly(oxyethylene) monomer unit.

2.2. Small-Angle X-ray Scattering (SAXS) Measurements. The structural evolution of doped siloxane−POE hybrids during the sol−gel transformation and aging at 60 °C was followed by in situ SAXS measurements using the synchrotron X-ray SAS beamline of LNLS (Campinas, Brazil). The studied samples were maintained inside a closed cell to avoid solvent evaporation. Measurements were started immediately after the europium-containing solution was added to the hybrid precursor.

The LNLS SAS beamline[25] is equipped with an asymmetrically cut and bent silicon(111) monochromator that yields a monochromatic (λ = 1.68 Å) and horizontally focused beam. A position-sensitive X-ray detector and a multichannel analyzer were used to record the SAXS intensity, $I(q)$, as a function of the modulus of the scattering vector q, $q = (4\pi/\lambda)\sin(\epsilon/2)$, where ϵ is the scattering angle. Because of the small size of the incident beam cross section at the detection plane, no mathematical desmearing of the experimental SAXS intensity function was needed. Each SAXS spectrum corresponds to a period of data collection of 300 s. The relative error for the SAXS intensity, $\Delta I(q)/I(q)$, was determined as the statistical error in the number of photons N collected during the 300-s collection time, $\Delta I(q)/I(q) = 2/N^{1/2}$. This statistical error was only significant for low scattering intensities, which are usually found in the high-q range ($q > 0.4$ Å^{-1}). The parasitic scattering intensity from the air, the slits, and the windows was subtracted from the total intensity. This scattering intensity was much weaker than that produced by the samples except over the asymptotic high-q range.

A first examination of the experimental SAXS results led us to propose, as in previous investigations of related systems, a two-level model for the structure of the studied hybrids (Figure 1). The relevant structure parameters were determined by fitting a theoretical function to the experimental SAXS curves. A nonlinear least-squares refinement procedure was used that also yields the errors in terms of the best-fit quality.

3. Method of SAXS Analysis

3.1. Scattering by Colloidal Particles Embedded in a Homogeneous Matrix. A simple structural model for isolated colloidal particles embedded in a homogeneous matrix is a two-electron-density system composed of a diluted set of identical homogeneous spheres spatially distributed at random. For this model, the SAXS intensity is given by the square of the form factor of the sphere, $\theta(q)$.[26] At high q, $P(q) = [\theta(q)]^2$ exhibits an oscillatory behavior. In real materials, the particles are often not perfectly spherical and/or do not all have the same radius. In these cases, the oscillations at high q are smeared out, and the Porod law [$I(q) = B/q^4$] holds.[27]

The scattering intensity produced by colloidal particles has an asymptotic behavior at low q described by the Guinier law, $I(q) = I(0)\exp(-R_g 2q^2/3)$, where R_g is the radius of gyration of the particles.[26] Beaucage[23] proposed an equation for the intensity scattered by a dilute set of approximately equal and homogeneous particles that exhibits Guinier and Porod[27] asymptotic behaviors at low and high q, respectively. This equation is given by

$$I(q) = NP(q) = G\exp\left(\frac{-q^2R_g^{\,2}}{3}\right) + B\{[\mathrm{erf}(qR_g/\sqrt{6})]^3/q\}^4 \quad (1)$$

The parameter G in eq 1 is given by[23]

$$G = NV^2(\rho_p - \rho_m)^2 \quad (2)$$

where ρ_p and ρ_m are the average electron densities of the particles and the matrix, respectively; V is the particle volume; and N is the number of particles per unit volume.[26] The asymptotic trend at high q corresponding to Porod's law is given by[27]

$$I(q) = B/q^4 \quad (3)$$

where

$$B = 2\pi(\rho_p - \rho_m)^2 S \quad (4)$$

with S being the interface area between the particles and matrix per unit volume. For spherical particles, the quotient B/G is given by

$$B/G = (81/50)/R_g^4 \quad (5)$$

If the colloidal particles are spatially correlated, the SAXS intensity is given by[23,27]

$$I(q) = NP(q)\, S(q) \quad (6)$$

where $NP(q)$ is given by eq 1 and $S(q)$ is the structure function accounting for the short-range order or spatial correlation of the particles.

Using Born−Green theory, Beaucage et al.[23] proposed a semiempirical structure function for a set of dense spheres surrounded by light spherical shells in contact given by

$$S(q) = 1/[1 + k\theta(q)] \quad (7)$$

where k is a packing factor and $\theta(q)$ is given by

$$\theta(q) = 3[\sin(qd) - qd\cos(qd)]/(qd)^3 \quad (8)$$

where d is the average interparticle distance. The packing factor k is equal to $8V/V_0$, where V is the average "hard-core" volume and V_0 is the average volume available to each sphere.

Equation 6 with $NP(q)$ and $S(q)$ defined by eqs 1 and 7, respectively, applies to systems composed of spheres in contact, with each sphere consisting of a hard core and an external shell with an average radius $R' = d/2$. This model seems to be suited, as a first approximation, to our hybrids composed of siloxane particles (the hard core) surrounded by soft (polymeric) shells.

3.2. Scattering by Colloidal Particles Confined in Small Segregation Domains. An analysis of our SAXS results led us to the conclusion that the primary siloxane clusters concentrate in rich domains embedded in a cluster-depleted matrix. This effect of phase separation induces the formation of a two-level hierarchical structure like that illustrated in Figure 1. Assuming that the internal spatial distribution of siloxane clusters is not correlated with the overall shape and size of the coarse domains, the X-ray scattering intensity produced by the primary particles (eq 6) and by the secondary domains, $[I(q)]_2$, are additive.[28] This should be considered only as a first approximation when the domains are not much larger than the primary clusters. For secondary domains with sizes of several hundred angstroms, only the outer part of $[I(q)]_2$ contributes significantly to the total scattering intensity within the q range of our experimental setup ($q > 0.02$ Å^{-1}). The asymptotic intensity of $[I(q)]_2$ generally exhibits a q dependence given by

$$[I(q)]_2 = A/q^\alpha \quad (9)$$

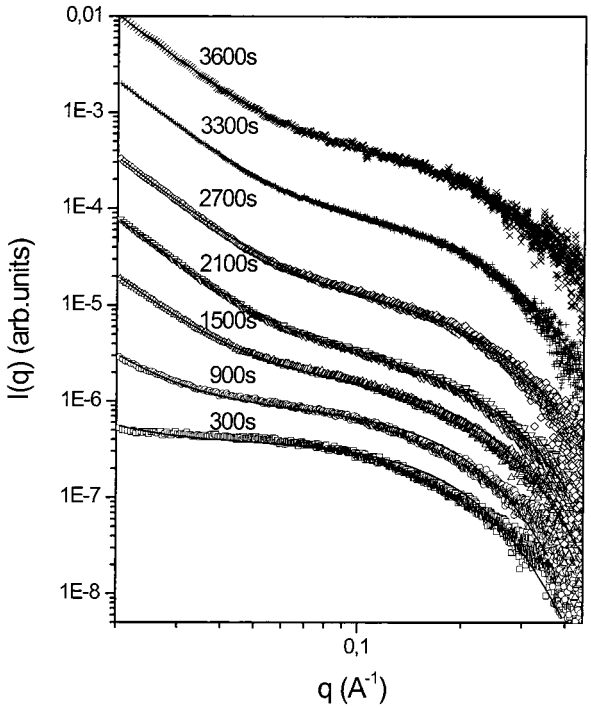

Figure 2. Experimental SAXS intensity curves (symbols) and fitted functions (solid lines) corresponding to a siloxane−POE hybrid with low europium content ($n = 80$) for the different indicated times. The curves are vertically displaced for clarity.

where A and α are constant parameters. The value of the exponent α is equal to 4 for globular particles with sharp interfaces (eq 4). For fractal objects and for objects with fractal interfaces or very anisotropic shapes, α is smaller than 4. Under this assumption, the total scattered intensity $[I(q)]_T$ for the proposed two level structure model is given by

$$[I(q)]_T = NP(q)\, S(q) + A/q^\alpha \quad (10)$$

Equation 10 with $S(q)$ given by eq 7 applies to systems composed of coarse domains that contain spatially correlated small clusters. If the siloxane clusters are weakly correlated, the same equation with $S(q) \approx 1$ holds.

4. Results

The SAXS intensity curves corresponding to $U(600)_{80}$ siloxane−POE hybrids with low $[U(600)_{80}Eu(CF_3SO_3)_3]$ ($n = 80$) and high $[U(600)_{25}Eu(CF_3SO_3)_3]$ ($n = 25$) Eu^{3+} contents are plotted in Figures 2 and 3, respectively. The different features of the scattering intensity curves corresponding to both types of samples will be discussed separately.

4.1. Hybrids with Low Europium Contents. The SAXS intensity $I(q)$ produced by the low-Eu^{3+}-doped $U(600)_{80}$ siloxane−POE hybrid, maintained at 60 °C for different periods of time up to 3600 s, is plotted in Figure 2. This time interval includes the initial aggregation in the sol ($t < 2700$ s), the sol−gel transformation and the gel aging process (2700 s $< t <$ 3600 s).

During the initial steps of the process ($t \leq 300$ s), the experimental SAXS intensity curves $I(q)$ were well fitted, as can be seen in Figure 2, by the theoretical function given by eq 10 with $S(q) = 1$ and $A \approx 0$. The fitted curve (continuous lines) agrees with the experimental data to within ±5%. This implies that, during the initial stages, the studied system can be well described by a simple model of spherical nanoparticles embed-

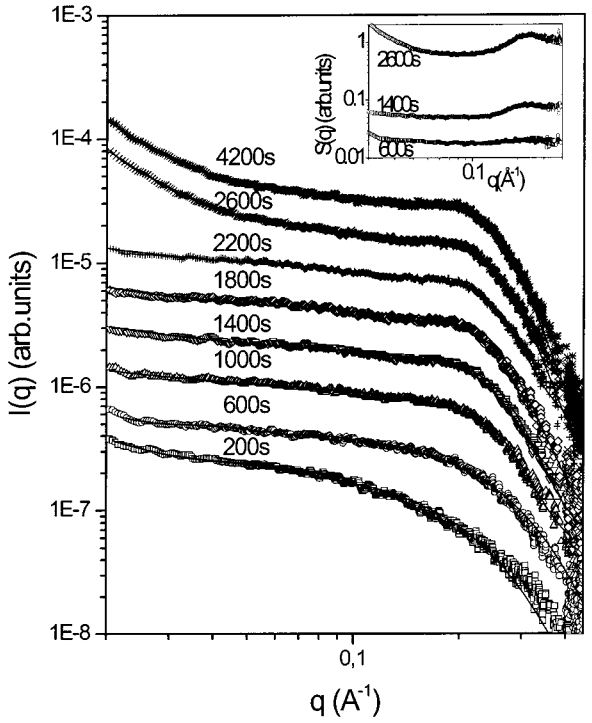

Figure 3. Experimental SAXS intensity curves (symbols) and fitted functions (solid lines) corresponding to a siloxane−POE hybrid with high europium content ($n = 25$) for the different indicated times. The curves are vertically displaced for clarity. The inset shows the structure factor $S(q)$ corresponding to initial (600 s), intermediate (1400 s) and final (2600 s) stages of the sol−gel transformation.

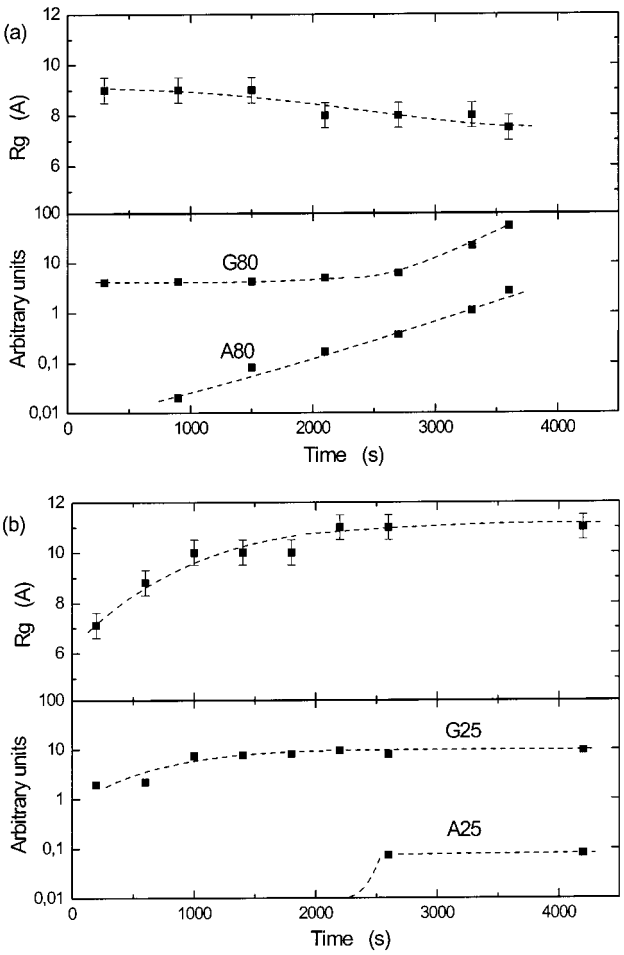

Figure 4. Time dependence of the radius of gyration of siloxane clusters, R_g, and parameters G and A (eq 10) corresponding to (a) siloxane−POE hybrids with a low Eu content ($n = 80$) and (b) siloxane−POE hybrids with a high Eu content ($n = 25$). The dashed lines are guides for the eyes.

ded in a homogeneous matrix. As the only chemical reaction occurring in the sol is the hydrolysis and condensation of the silicon species of the hybrid precursor and the electronic density of siloxane particle is much higher than that associated with PEO and the solvents (essentially composed of carbon and hydrogen atoms), we have concluded that the particles that are responsible for the X-ray scattering are clusters of siloxane groups chemically bonded to the ends of the POE chains. These clusters are homogeneously dispersed in a polymer−solvent matrix.

At more advanced stages of the sol−gel transformation, the scattering intensity curves plotted in Figure 2 contain an additional contribution at very small q, which suggests that the structure exhibits two levels, as illustrated in Figure 1. We have, in this case, a contrast in electron density between the siloxane clusters and the matrix mainly composed of folded polymer chains inside the cluster-rich domains (first level) and between the coarse domains and a cluster-depleted matrix composed of unfolded polymer chains, non-hydrolyzed precursor, and solvent (second level). Taking into account the assumptions mentioned in section 3.2, we assigned the SAXS intensity at medium and high q ($q > 0.04$ Å^{-1}) to the first level of electron density contrast and the additional contribution observed in the low-q range ($q \leq 0.04$ Å^{-1}) to the second one.

The contribution to the SAXS intensity from the siloxane-cluster-rich domains within the studied q range is characterized by the factor A and the exponent α (eq 9). At the beginning of the process this contribution is small, so we have determined the exponent α from the SAXS intensity curves at long times ($\alpha = 2.8$) and assumed that this value is approximately invariant throughout the process. Under this assumption, $A(t)$ yields a rough estimate of the time variation of the volume fraction occupied by the siloxane-rich domains. From the Guinier plots of the scattering intensity at small q, we could establish only an estimate of the lower limit of the average diameter D_{min} of the coarse domains ($D \geq 200A$). A more precise description of the structure of the secondary domains requires additional SAXS measurements at smaller q values ($q \ll 0.02A$).

The structural parameters R_g, G, and A of eq 10 were determined by a nonlinear least-squares refinement procedure. The results are plotted as functions of time in Figure 4a. The experimental results indicate that, at the very beginning of the process, during the sol−gel transition ($t < 2700$ s), and also during gel aging ($t > 2700$ s), the average radius R_g of the primary siloxane particles remains approximately constant around 9 Å. This value is larger than that previously determined for undoped siloxane−POE hybrids.[12,20] This reveals that low europium doping ($n = 80$) accelerates the hydrolysis and condensation reactions between the silicon species located at polymer chain ends. This effect has already been observed in other sol−gel-derived materials containing different salts[1] and is attributed to Eu^{3+} ions decreasing the electrostatic repulsion between the silicon species.

A continuous increase in the $G(t)$ function during gelation is apparent in Figure 4a. Taking into account eq 2 and considering that (i) the electronic density contrast ($\rho_p - \rho_m$) between the primary siloxane nanoclusters and the matrix constituted of folded polymer chains (which eventually contains a low content of non-hydrolyzed precursor molecules and solvent) is expected

to be only slightly modified during the process and (ii) the average radius R and volume V of the siloxane clusters remain essentially constant, the increase in $G(t)$ indicates a progressive increase in the number N of siloxane clusters inside each domain. This effect occurs from the very beginning of the process until the final aging of the gel.

In all curves corresponding to $t > 300$ s, the already mentioned additional contribution to the SAXS intensity at low q ($q < 0.03$ Å^{-1}) is apparent (Figure 2). For these advanced stages, eq 10 with $S(q) = 1$ also fits well to experimental data, but in this case, the parameter A corresponding to the second-level structure has a nonvanishing value. The increasing trend of the $A(t)$ function, plotted in Figure 4a, reveals the progressive increase of the contribution to the scattering intensity at small q produced by the domains in which siloxane clusters are segregated. This suggests that the total volume of the coarse domains containing siloxane clusters progressively grows from the first stages until gel aging.

The good fittings of the theoretical eq 10 with $S(q) \approx 1$ to the experimental curves shown in Figure 2 suggest that the primary siloxane clusters inside the large secondary domains are not or are only very weakly spatially correlated.

4.2. Hybrids with High Europium Contents. The SAXS intensity curves $I(q)$ corresponding to a highly Eu^{3+}-doped sample $[U(600)_{25}Eu(CF_3SO_3)_3]$ ($n = 25$) during the whole sol−gel transformation ($0 < t \leq 2600$ s) and gel aging (2600 s $< t \leq 4200$ s) process are plotted in Figure 3.

The observation of the shapes of the experimental SAXS curves and the time dependence of R_g, G, and A obtained from the fitting procedure (Figure 4b) reveal two different regimes corresponding to (i) the initial stage of aggregation in the sol state ($t \leq 2200$ s) and (ii) the final stage of sol−gel transformation and gel aging ($t > 2200$ s).

During the first regime, the SAXS intensity given by eq 10 with a structure function $S(q) \neq 1$ defined by eq 7 fits the experimental data well (to within ±5%) over the whole q range.

The results plotted in Figure 4b indicate that the average radius of gyration R_g of the primary siloxane clusters in highly Eu^{3+}-doped hybrids is initially small and continuously increases, reaching a maximum value ($R_g \approx 11$ Å) close to the gel point. On the other hand, the function $G(t)$ also exhibits a continuous increase until $t = 2200$ s. This increase of $G(t)$ correlates well with the observed increase in siloxane cluster size and volume, as expected from eq 2.

The slow growth of the siloxane clusters in hybrids with high europium contents ($n = 25$) indicates that a high concentration of Eu^{3+} ions inhibits the polycondensation reactions between silicon species located at the polymer chain ends. This slow process of cluster growth was not observed for samples with low europium content ($n = 80$), where primary particles of about 9 Å are formed in the very first gelation stages (Figure 4b).

On the other hand, the spatial correlation of siloxane clusters increases during gelation, as suggested by the progressive growth of the interference peak in the structure function $S(q)$ (inset of Figure 3). This is also apparent in the results plotted in Figure 5, which illustrates the monotonic increase in the packing factor k and the sharp decrease of the average intercluster distance d for increasing time.

In the second regime, during the final stage of gelation ((2200 s $< t \leq 2600$ s) and gel aging (2600 s $< t \leq 4200$ s), the good agreement between the theoretical function described by eq 10 with $S(q) \neq 1$ and the features of the experimental data plotted in Figure 3 reveal the formation of secondary cluster-rich domains. The fact that these domains start to be formed only at the final gelation stage and the invariance of R_g, G, and A (Figure 4b) confirm that a high concentration of Eu^{3+} ions inhibits the polycondensation reactions between silicon species of the hybrid precursor.

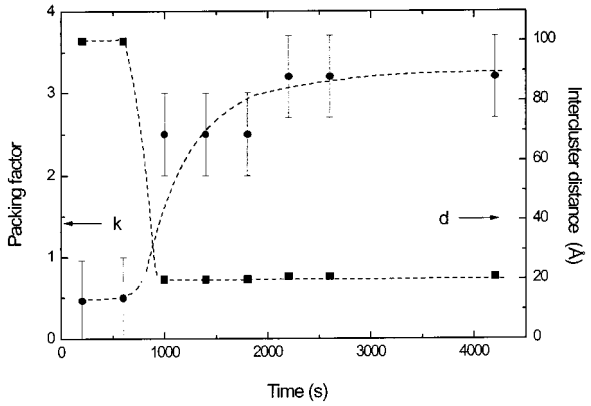

Figure 5. Time variation of the packing factor k and the average distance between siloxane clusters d corresponding to siloxane−POE hybrids with a high Eu content ($n = 25$). The dashed lines are guides for the eyes.

5. Discussion

The difference in the mechanism of sol−gel transformation and gel aging of $U(600)_{80}Eu(CF_3SO_3)_3$ (low Eu^{3+} content) and $U(600)_{25}Eu(CF_3SO_3)_3$ (high Eu^{3+} content) is coherent with the different natures of the coordination sites for europium cations observed in the dry gel of same composition.[22] In fact, in the $U(600)_n$ hybrids, the preferential coordination sites for the Eu^{3+} ions are the ether-type oxygens of the polymer as long as the Eu^{3+} content is kept low (n greater than 60). At higher Eu^{3+} doping levels, $n \leq 40$, a distinct local cation site environment involves the interaction of the europium ions with the urea carbonyl oxygens atoms at the siloxane−POE interface.[22] This should lead to steric hindrance of the motion of the silicon species located at the chain ends, which inhibits the polycondensation reactions.

The spatial correlation of siloxane clusters has already been observed during the drying of undoped siloxane−polyether hybrids.[18,19] This correlation was associated with an effect of polymer phase contraction induced by solvent evaporation, leading to a shortening of the average distance between siloxane clusters. Analogously, the progressive increase in spatial correlation of siloxane clusters during the gelation of $U(600)_{25}Eu(CF_3SO_3)_3$ samples can be associated with the volume contraction and consequent folding of the polymeric chains. This phenomenon can be attributed to the formation of −C═O−Eu^{3+}−O═C− cross-links between europium ions and carbonyl oxygens located in the extremities of different POE chains. In fact, for a high salt concentration, $n = 25$, there are approximately six available carbonyl oxygens for each cation. Ion coordination to a similar number of carbonyl groups has already been observed in europium-doped siloxane−POE dried gels containing polymer of higher molecular weight.[13,15,22] The presence of cross-links has independently been evidenced in siloxane−POE hybrids containing europium perchlorate at a similar doping level.[24] The formation of secondary cluster-rich domains observed during the final gelation stages increases the probability of occurrence of such cross-links, favoring the contraction of the polymer chains and thus increasing the spatial correlation of siloxane nanoparticles during sol−gel transformation.

To confirm the specific role of Eu in the cross-linking of polymer chains suggested by our experimental results, further neutron diffraction and/or NMR studies are required

6. Conclusion

Two different mechanisms are responsible for the sol−gel transformation and gel aging of europium-doped siloxane−POE nanocomposites. The first is the formation and growth of primary siloxane clusters, with a final average radius of gyration of around 10 Å, grafted to the extremities of the polymer chains. The second mechanism is the formation of rather large siloxane cluster-rich domains embedded in a cluster-depleted matrix.

The kinetics of the sol−gel transformation depends on the europium content. For low europium doping ($n = 80$), the growth of individual siloxane clusters is fast, and subsequently, the system evolves by increasing the size and/or number of the domains containing siloxane clusters. For high europium doping ($n = 25$), the polycondensation reaction is a slow process, and the growth of siloxane clusters is the preponderant mechanism of structural transformation during the gelation process. The segregation of siloxane clusters forming domains only occurs during the final stages of the sol−gel transition.

The formation of domains in which siloxane clusters concentrate is probably enhanced by the polycondensation reactions between siloxane groups that have not reacted during the first stages, promoting the folding of the polymer chains. This process is heterogeneous, forming a number of small cluster-rich domains embedded in a depleted matrix composed of unfolded chains and solvent.

Acknowledgment. The authors acknowledge the collaboration of LNLS staff during the SAXS experiments and the financial support from Brazilian (FAPESP, CAPES, and PRONEX) and Portuguese (ICCTI and FCT−PRAXIS/P/CTM/13175/98) agencies.

References and Notes

(1) Brinker, C. J.; Scherrer, G. W. *Sol−Gel Science, The Physics and Chemistry of Sol−Gel Processing*; Academic Press: New York, 1990.
(2) Novak, B. *Adv. Mater*. **1993**, *5*, 422.
(3) Wen, J.; Wilkes, G. L. *Chem. Mater*. **1996**, *8*, 1667.
(4) Judeinstein, P.; Sanchez, C. *J. Mater. Chem*. **1996**, *6*, 511.
(5) Sanchez, C.; Ribot, F.; Lebeau, B. *J. Mater. Chem*. **1999**, *9*, 35.
(6) (a) *Sol−Gel Optics I*; Mackenzie, J. D., Ulrich, D. R., Eds.; SPIE Symposia Proceedings 328; SPIE: Washington, DC, 1990. (b) *Sol−Gel Optics II*; Mackenzie, J. D., Ed.; SPIE Symposia Proceedings 1758; SPIE: Washington, DC, 1992. (c) *Sol−Gel Optics III*; Mackenzie, J. D., Ed.; SPIE Symposia Proceedings 2288; SPIE: Washington, DC, 1994;
(7) Pope, E. J. A. *J. Sol−Gel Sci. Technol*. **1994**, *2*, 717.
(8) Law, H.; Tou, T. *Appl. Opt*. **1998**, *37*, 5694.
(9) Carlos, L. D.; De Zea Bermudez, V.; Silva, M. M.; Duarte, M. C.; Silva, C. J. R.; Smith, M. J.; Assunção, M.; Alcácer, L. *Physics and Chemistry of Luminescent Materials VI*; Ronda, C., Welker, T., Eds.; The Electrochemical Society Proceedings: San Francisco, CA, 1998; p 352.
(10) De Zea Bermudez, V.; Carlos, L. D.; Duarte, M. C.; Silva, M. M.; Silva, C. J.; Smith, M. J.; Assunção, M.; Alcácer, L. *J. Alloys Compd*. **1998**, *21*, 275.
(11) Ribeiro, S. J. L.; Dahmouche, K.; Ribeiro, C. A.; Santilli, C. V.; Pulcinelli, S. H. *J. Sol−Gel Sci. Technol*. **1998**, *13*, 427.
(12) Carlos, L. D.; De Zea Bermudez, V.; Sá Ferreira, R. A.; Marques, M.; Assunção, M. *Chem. Mater*. **1999**, *11* (3), 581.
(13) Carlos, L. D.; Sá Ferreira, R. A.; de Zea Bermudez, V.; Molina, C.; Bueno, L. A.; Ribeiro, S. J. L. *Phys. Rev. B*. **1999**, *60*, 10042.
(14) Bekiari, V.; Lianos, P.; Judeinstein, P. *Chem. Phys. Lett*. **1999**, *307*, 310.
(15) Carlos, L. D.; Messaddeq, Y.; Brito, H. F.; Sá Ferreira, R. A.; de Zea Bermudez V.; Ribeiro, S. J. L. *Adv. Mater*. **2000**, *12*, 594.
(16) Bekiari, V.; Lianos, P.; Stangar, U. L.; Orel, B.; Judeinstein, P. *Chem. Mater*. **2000**, *12*, 3095.
(17) Carlos, L. D.; Sá Ferreira, R. A.; de Zea Bermudez, V.; Ribeiro, S. J. L. *Adv. Funct. Mater*., in press.
(18) Dahmouche, K.; Santilli, C. V.; Chaker, J. A.; Pulcinelli, S. H.; Craievich, A. F. *Jpn. J. Appl. Phys*. **1999**, *38*, 172.
(19) Chaker, J. A.; Dahmouche, K.; Santilli, C. V.; Pulcinelli, S. H.; Craievich, A. F. *J. Sol−Gel Sci. Technol*. **2000**, *19*, 137.
(20) , Dahmouche, K.; Santilli, C. V.; Pulcinelli, S. H.; Craievich, A. F. *J. Phys. Chem. B* **1999**, *103*, 4937.
(21) Dahmouche, K., Santilli, C. V.; da Silva, M.; Ribeiro, C. A.; Pulcinelli, S. H.; Craievich, A. F. *J. Non-Cryst. Solids*. **1999**, *247*, 108.
(22) Dahmouche, K.; Carlos, L. D.; Sá Ferreira, R. A.; Santilli, C. V.; de Zea Bermudez, V.; Craievich, A. F. *J. Mater. Chem*. **2001**, *11*, 3249.
(23) Beaucage, G.; Ulibarri, T. A.; Black, E. P.; Schaefer, D. W. Hybrid Organic−Inorganic Composites. *ACS Symp. Ser*. **1995**, *97*, *585*.
(24) Molina, C.; Ribeiro, S. J. L.; Dahmouche, K.; Santilli, C. V.; Craievich, A. F. *J. Sol−Gel Sci. Technol*. **2000**, *19*, 615.
(25) Kellermann, G.; Vicentin, F.; Tamura, E.; Rocha, M.; Barbosa, A. L.; Craievich, A.; Torriani, I. *J. Appl. Crystallogr*. **1997**, 30, 880.
(26) Guinier, A.; Fournet, G. *Small-Angle X-ray Scattering of X-rays*; John Wiley and Sons: New York, 1955; p 55.
(27) Glatter, O.; Kratky, O.; *Small-Angle X-ray Scattering*; Academic Press: New York, 1982.
(28) Guinier, A. *Théorie et Téchnique de la Radiocristallographie*; Dunod: Paris, 1964.